Feasibility of whole-body diffusion-weighted MRI for detection of primary tumour, nodal and distant metastases in women with cancer during pregnancy: a pilot study.

Sileny N. Han, PhD[1], Frédéric Amant, PhD[1,2], Katrijn Michielsen, MSc[3], Frederik De Keyzer, MSc[3], Steffen Fieuws, PhD[4], Kristel Van Calsteren, PhD[1], Raphaëla C. Dresen, PhD[3], Mina Mhallem Gziri, PhD[5], Vincent Vandecaveye, PhD[3].

[1]*Departments of Obstetrics and Gynaecology, University Hospitals Leuven, Leuven, Belgium;*

[2]*Center for Gynaecological Oncology Amsterdam (CGOA), Antoni van Leeuwenhoek-Netherlands Cancer Institute; Amsterdam, the Netherlands;*

[3]*Radiology, University Hospitals Leuven, Leuven, Belgium;*

[4]*Department of Public Health and Primary Care, KU Leuven – University of Leuven & Universiteit Hasselt, Leuven, Belgium;*

[5]*Obstetrics and Gynaecology, Cliniques Universitaires Saint-Luc, Woluwe Saint-Lambert, Belgium*

Corresponding author

Prof. Dr. Frédéric Amant

Address: University Hospitals Leuven, Herestraat 49, B-3000, Leuven, Belgium

E-mail: frederic.amant@uzleuven.be

Phone : 0032 16 344252

Fax : 0032 16 344629

Abstract

Objectives: To evaluate the feasibility of whole-body diffusion weighted magnetic resonance imaging (WB-DWI/MRI) for detecting primary tumour, nodal and distant metastases in women with cancer during pregnancy.

Methods: Twenty pregnant patients underwent WB-DWI/MRI additionally to conventional imaging in this prospective single centre study. Reproducibility of WB-DWI/MRI between 2 readers was evaluated using Cohen's κ statistics and accuracy was compared to conventional imaging for assessing primary tumor site, nodal and visceral metastases.

Results: Both WB-DWI/MRI readers showed good to very good agreement for lesion detection (primary lesions: κ=1; lymph nodes: κ=0.89; distant metastases: κ=0.61). Eight (40%) patients were upstaged after WB-DWI/MRI. For nodal metastases, WB-DWI/MRI showed 100% (95% CI:83.2-100) sensitivity for both readers with specificity of 99.4% (95% CI:96.9-100) and 100% (95% CI:80.5-100) for reader 1 and 2 respectively.

For distant metastases, WB-DWI/MRI showed 66.7% (95% CI:9.4-99.2) and 100% (95% CI:29.2-100) sensitivity and specificity of 94.1% (95% CI:71.3-99.9) and 100% (95% CI: 80.5-100) for reader 1 and 2 respectively.

Conventional imaging showed sensitivity of 50% (95% CI:27.2-) and 33.3% (95% CI:0.8-90.6); specificity of 100% (95% CI:98-100) 100% and (95% CI:80.5-100), for nodal and distant metastases respectively.

Conclusions: WB-DWI/MRI is a promising single-step non-invasive imaging method for women with cancer during pregnancy.

Key words: Magnetic resonance imaging, diffusion magnetic resonance imaging, cancer, pregnancy, staging.

Key points:

- In our study, WB-DWI/MRI was more accurate than conventional imaging during pregnancy.
- WB-DWI/MRI helps to accurately assess patients with cancer diagnosed during pregnancy.

Introduction

Cancer is diagnosed during pregnancy in approximately 1:1000-2000 pregnancies [1]. The incidence rate is expected to rise in the coming years due to a rising trend of delaying pregnancy to a later age [2]. The most common types of cancer diagnosed during pregnancy include breast cancer, haematological malignancies, melanoma and cervical uterine cancer [3]. A standardized approach is often lacking and poses significant conflicts between maternal benefit and fetal risk. Fear of fetal radiation exposure often leads to suboptimal staging. Diagnostic or radionuclide scans should not be withheld from pregnant patients if a scan is medically indicated for the benefit of the mother or the fetus [4]. However, ionizing radiation such as computed tomography (CT) and fluorodeoxyglucose positron emission tomography/CT (FDG-PET/CT) should be avoided whenever possible during pregnancy.[5] The most obvious methods able to avoid radiation are ultrasound and magnetic resonance imaging (MRI). Both modalities are mainly used for detailed local-regional disease assessment or a specific organ (e.g. liver). While providing excellent information on the organ system examined, this approach often requires multimodality and multistep diagnostics. MRI has a number of advantages for oncological staging as the technique allows more reproducible evaluation of entire organ systems and – more recently - whole body (WB) evaluation. Moreover, MRI allows evaluation of functional tissue properties through the use of diffusion weighted imaging (DWI) without the need for a contrast-agent. DWI visualizes tumoral lesions by combining heavy diffusion-weighting and background signal suppression of organs, blood vessels and body fluids [6]. DWI generates image contrast by probing differences in water molecule movement (Brownian molecular motion) between tissues with different cellularity, extracellular microstructure, and microcirculation. The degree of impediment or restriction of water diffusion in biologic tissue increases with increasing tissue cellularity. The more water molecule movement is restricted; the brighter lesions appear at

DWI with heavy diffusion weighting up to b1000. This results in high signal contrast with tumoral lesions being depicted as bright foci in contrast to the suppressed background tissue [7].

Technological innovations have made whole-body diffusion weighted magnetic resonance imaging (WB-DWI/MRI) a time-efficient scanning method, with thin slice acquisition, millimetre-sized spatial resolution and robust performance. These advantages explain its promising development for tumor screening and staging [6,8,9]. There is already a decent body of evidence showing that DWI has satisfying sensitivity and specificity for the detection of nodal and visceral metastases, including peritoneal, liver, bone and pleural involvement [10-12].

We hypothesize that WB-DWI/MRI is a radiation-free single-step modality for diagnosis and staging of cancer during pregnancy, while reducing the need for multimodality, invasive staging. The objective of our study is to evaluate the feasibility of whole-body diffusion weighted magnetic resonance imaging (WB-DWI/MRI) for detecting primary tumour, nodal and distant metastases in women with cancer during pregnancy.

Materials and Methods

Patients

Approval for this prospective single centre academic pilot study was obtained from the local institutional ethics review board. Written informed consent was required. The inclusion criterion was clinical diagnosis of cancer during pregnancy. Exclusion criteria were previous history of malignancy prior to conception and contra-indications to MRI (e.g. pacemaker, claustrophobia).

Between September 2012 and January 2015, 22 consecutive pregnant patients (mean age 35.8, range 29-40 years) with suspected malignancy were invited to participate in this study, two patients declined due to claustrophobia. Twenty patients underwent WB-DWI/MRI in addition to routine staging procedures including diagnostic clinical/laboratory, surgical and imaging work-up. Extent and types of routine clinical staging modalities – hereafter called conventional staging - were chosen by the treating physician. The conventional staging methods compared to WB-DWI/MRI are depicted in Table 1. TNM-classification [13] and Ann-Arbor classification in case of suspected lymphoma was used for staging.

The study was designed that - after conclusion of all diagnostic work-up - metastases relevant for therapeutic decisions detected by WB-DWI/MRI were disclosed to the treating physician in order to allow for biopsy or correlative imaging to conclude the diagnostic process and in order to adapt treatment when necessary.

Imaging technique: Whole body diffusion MRI

All patients underwent WB-DWI/MRI at 3 Tesla field-strength with parallel radiofrequency transmission and phased-array head–neck and surface coils (Ingenia Philips Medical Systems). The MRI-system has a bore diameter of 70 cm, which is helpful to comfortably scan pregnant patients. Free breathing short-tau inversion recovery (STIR) WB-DWI/MRI

was acquired in the transverse plane at b0 and b1000 sec/mm2, from the head to below the pelvis. Whole body images were generated automatically by the scanners software by reconstructing multiplanar reformatted (MPR) coronal and sagittal WB-DWI/MRI images from the transverse b1000 images.

For anatomical reference for visceral organs and lymph nodes, whole body coronal non-fat suppressed T2-weighted (w) single-shot turbo spin-echo (SS-TSE) and a thoracic 3D T1-weighted sequence were used. When indicated for skeletal evaluation, a T1w TSE sequence over the spine and pelvis was added. Detailed pulse sequence parameters are provided in Table 2. No oral or intravenous contrast was given.

Image interpretation: WB-DWI/MRI

WB-DWI/MRI was evaluated by two abdominal radiologists (10 and 2 years of experience, respectively). Observers were blinded to all information regarding the other imaging tests, clinical, laboratory and pathological findings but were aware of the clinical diagnosis of cancer.

As previously described, at WB-DWI/MRI, primary lesions and visceral metastases were recorded when nodular or mass-like b1000 hyperintensity was present, not attributable to T2 shine-through – defined as fluid-like hyperintensity at T2 weighted imaging - or physiological impeded diffusion in anatomical structures. Skeletal metastases were recorded when b1000 hyperintense lesions were present, correlated to T1 hypo-intense lesions and not attributable to T2 shine-through at T2 weighted imaging. Lymph nodes were qualitatively assessed on the basis of b1000 SI; lymph nodes showing (heterogeneous) b1000 SI equal to or higher than the solid component of the primary tumor as compared with surrounding lymph nodes were considered malignant, irrespective of nodal size. In the absence of a primary tumour or suspected lymphoma, lymph nodes showing (heterogeneous) b1000 SI higher than the

surrounding lymph nodes were considered malignant [6] Co-registered anatomical MR-images were for anatomical correlation of DWI findings, to classify physiological b1000 hyperintensity and lesions smaller than 4 mm with intermediate b1000 SI due to possible partial volume effects. [6]

WB-DWI/MRI assessment was divided in the following anatomical subsites: the primary tumor site, including assessment of location and size; nodal regions, including Waldeyer' ring, cervical region (left and right), supraclavicular region (left and right), mediastinum, pulmonary hilum, axillar region (left and right), retrocrural region, retroperitoneal region, iliac region (left and right) and inguinal region (left and right) and distant sites including the skeleton (axial and non-axial), visceral organs (liver, lungs, kidneys, pancreas, spleen) and surface lining organs (pleura and peritoneum).

Reference standard

Histopathology, either at staging laparotomy, diagnostic laparoscopy, core biopsy or fine needle aspiration cytology, was primarily used to confirm detected lesions at primary, nodal and distant potentially metastatic sites whenever possible.

For disease sites marked negative at WB-DWI/MRI or conventional staging and for lesions without histopathological correlation, post-treatment patient follow-up and remission status was used as reference standard to exclude development of metastatic lesions. For this purpose, the following imaging criteria were defined: lesions appearing significantly larger (at least 20% increase) during follow-up or showing a significant decrease after chemotherapy (at least 30% decrease) were considered to be true positive. Lesions initially detected that had resolved without therapy were considered false positive. Sites that were initially classified as negative but unequivocally showed tumor at follow-up examinations were considered false negative. Sites, initially designated as negative and not showing any tumor during follow-up

were considered true negative. Clinical and follow-up information was collected from the INCIP-registration study (www.cancerinpregnancy.org).

Statistical analysis

Analyses were performed using SAS software (version 9.2, SAS System for Windows). Conventional staging and WB-DWI/MRI based staging was compared for sensitivity, specificity, accuracy, positive (PPV) and negative predictive values (NPV) for detection of primary tumor, nodal and distant metastases. Exact 95% confidence intervals (CIs) based on the binomial distribution are reported for all diagnostic indices (sensitivity, specificity, PPV, NPV, accuracy). Kappa statistics was used to quantify inter-rater reliability. Since the sample size is small when primary lesions and distant metastases are considered, a confidence interval based on the exact bootstrap distribution for the kappa value is reported instead of the asymptotic one [14]. Note that we have adapted their SAS program to handle the presence of zero values.

Since for many patients multiple sites have been assessed, the CIs for the diagnostic indices and the kappa value are too liberal in the evaluation of the nodal metastases. To adjust the CI for the diagnostic indices, an approach based on the ratio estimator for the variance of clustered binary data was used [15]. However, this approach is only asymptotically valid and no CI is obtained when the diagnostic index equals 100%. Therefore, to be conservative, we have decided to report in each setting the confidence limits from the approach yielding the widest one. The CI for the kappa on the nodal metastases is adjusted by multiplying the asymptotic variance by the design effect. The latter equals 1+rho*(m-1), where rho equals the intra-class coefficient calculated on the agreement and m the average number of sites (=10) [16]. With rho=0.036, the design effect equalled 1.324 in the current study.

Results

Patients

Ten of the 20 included patients had breast cancer (50 %), 3 Hodgkin lymphoma (15%), 2 cervical uterine cancers (10%), 1 ovarian borderline tumor (5%), 2 colon cancers (10%), 1 lung cancer (5%) and 1 a conjunctival malignant tumor (5%). Disease extent and staging according to the reference standard and according to WB-DWI/MRI for both readers is displayed in Table 3.

Three patients were referred for staging after primary tumor resection, with the question for residual tumor: one patient with cervical uterine cancer after conisation, one patient with colon cancer after appendectomy and caecal resection and one patient with conjunctival tumor.

Comparison of conventional staging with WB-DWI/MRI

In total, 8/20 (40%) of patients were upstaged after WB-DWI/MRI. Comparative sensitivities, specificities, accuracies, PPVs and NPVs of conventional staging and WB-DWI/MRI for both readers, are shown in Table 4.

Identical to conventional staging, WB-DWI/MRI allowed correct identification of the primary tumor in all but 1 patient.

For nodal staging, conventional staging underestimated clinically relevant metastatic extent in 5 patients, all with breast cancer (Figure 1). Three of these 5 patients were presumed node negative based on conventional staging. In 1 patient WB-DWI/MRI additionally detected a supraclavicular adenopathy. WB-DWI/MRI allowed better detection of involved nodal disease sites in the 3 lymphoma patients which did not lead to significant change of stage. Reader 1 falsely assigned an ipsilateral hilar lymph node as metastatic in the patient with lung cancer.

Of the 3 patients with distant metastases, conventional staging correctly detected skeletal metastases in 1 patient; WB-DWI/MRI reader 1 correctly identified distant metastases in 2 patients and WB-DWI/MRI reader 2 detected distant metastases in all 3 patients (Figure 2, patient with colon cancer; and Figure 3, patient with cervical cancer). In a breast cancer patient, WB-DWI/MRI reader 1 identified a b1000 hyperintense lesion at DWI in the rib requiring additional CT for definitive diagnosis of skeletal hemangioma. To allow comparison in this study, this was considered a false positive finding at WB-DWI/MRI for reader 1.
Both WB-DWI/MRI readers showed good to very good agreement for lesion detection [primary lesions: Kappa (95% CI) = 1.00 (0.44 -1.00); lymph nodes: Kappa (95% CI) = 0.90 (0.78; 1.00); distant metastases: Kappa (95% CI) = 0.61 (-0.07; 1.00)].

Gestational outcome

Four patients were staged during the first trimester of pregnancy (between 7 weeks (w) 2/7 days (d) and 8w 6/7d), of which one patient with a Hodgkin lymphoma decided to terminate the pregnancy before starting treatment, and another patient had a missed abortion at 10w 2/7d (histopathological examination of the curettage material revealed a partial mola hydatidiformis). Sixteen patients were staged during the second and third trimester of pregnancy, of which one patient with a monochorionic diamniotic twin pregnancy developed a twin-to-twin transfusion syndrome. Chorioamnionitis and intrauterine death of both fetuses at 18w occurred after fetal surgery. Fifteen neonates were born healthy and without congenital anomalies (median gestational age at birth 37w 5/7d (range 33w 2/7d to 40w 0/7d)).

Discussion

The findings of this pilot study demonstrate the feasibility of WB-DWI/MRI for staging of women with cancer during pregnancy. With good to very good observer agreement, WB-DWI/MRI allowed accurate identification of the primary tumor site and more accurate staging of nodal and distant metastases compared to conventional staging.

The improved detection of nodal metastases by WB-DWI/MRI was most beneficial in the patients with breast cancer. In one patient, an unknown supraclavicular lymphadenopathy was detected; changing treatment from upfront surgery to neo-adjuvant chemotherapy and in 3 other patients the better detection of axillary nodal involvement could have enabled upfront axillary lymphadenectomy, potentially sparing sentinel lymph node biopsy. As patients with lymph node metastases have a poorer prognosis compared to node-negative patients (10-years recurrence risk of 70% and 15-30% respectively), the ability to detect small nodal metastases by DWI may enable earlier stratification of patients at risk of recurrence or requiring more aggressive treatment [17,18].

Separate studies have investigated DWI for regional nodal staging in breast cancer using both qualitative visual and quantitative assessment with reported sensitivities between 72.4% and 97% with specificities between 54.4% and 91.7% [19-23].

In comparison, reported sensitivities and specificities for ultrasound are between 26.4% and 92% and specificities of 55.6%–98.1% [24].

Importantly, the increase of sensitivity by DWI may come with a decrease of specificity. This was only of minor degree in our patient series. WB-DWI/MRI poses particular potential challenges towards nodal staging, due to the potentially high workload of manual region of interest (ROI) delineation and the possible lack of reproducibility and stable threshold of apparent diffusion coefficient (ADC) measurements if quantitative evaluation would be performed for nodal characterization.[6] Therefore, we opted to assess lymphadenopathies in

a qualitative way. The high accuracy obtained in this patient series using predetermined qualitative interpretative criteria for DWI relating the b1000 SI of nodal disease to that of the primary tumour and surrounding lymph nodes is in line with previous studies in abdominopelvic and pulmonary cancers [6,25].

WB-DWI/MRI enabled better description of total nodal disease involvement in the 3 lymphoma patients, but this did not lead to substantial change in staging. In literature, arguments both favoring and questioning MRI for staging lymphoma during pregnancy are found. As the vast majority of patients are initially treated with chemotherapy, it has been proposed to limit imaging procedures to chest X-ray and ultrasound [26]. However, correct staging and clinical management aids to optimize long-term survival [27]. Importantly, ultrasound results are not always conclusive in lymphoma due to the low sensitivity for detecting abdominal lymphadenopathies while the superimposition of air and bone inhibits ultrasonographic assessment of the mediastinum [28]. WB-DWI/MRI has shown excellent agreement up to 99.4% with FDG-PET/CT for staging lymphoma and is indicated as a non-irradiating alternative to FDG-PET/CT for staging lymphoma and other malignancies including lung cancer [9, 25]. Contrary to ultrasound/chest X-ray, WB-DWI/MRI allows for a maximal staging effort similar as for non-pregnant patients and also better exclusion of other primary tumors than lymphoproliferative disease in the diagnosis process.

With slightly lower interrater agreement compared to nodal staging, WB-DWI/MRI enabled better detection of distant metastases at primary diagnosis compared to conventional staging. Recent studies have demonstrated a good diagnostic performance of WB-DWI/MRI for detecting distant metastatic spread, equivalent to FDG-PET/CT [12]. WB-DWI/MRI has shown particularly high diagnostic value for assessing hepatic and peritoneal metastases in digestive and ovarian cancer compared to contrast-enhanced MRI, contrast-enhanced CT or

FDG-PET/CT [6,29,30]. WB-DWI/MRI also has shown higher accuracy than bone scintigraphy for detecting skeletal metastases [31].

The safety profile of MRI towards the fetus is subject to debate and contributes to a reluctance to use MRI for first-line clinical assessment during pregnancy. Assumed concerns include potential heating effects from radiofrequency pulses and acoustic noise possibly related to fetal growth restriction, premature birth and hearing impairment. A retrospective case-control study in 751 neonates did not show impaired hearing or low birth weight secondary to MRI exposure, confirming findings of previous case series [32-35].

To date, no studies have indicated that any pulse sequences at 1.5 Tesla field-strength cause significant increases in temperature [36]. 3 Tesla MRI has the benefit of better signal-to-noise ratio, thereby improving diagnostic quality or decreasing imaging time while maintaining high image quality. A recent study evaluating intra-uterine heating effects by 3 tesla MRI in pregnant miniature pigs showed only minimal temperature increase when limiting scan time to 30 minutes and using low SAR sequences but cautioned for heating effects when using prolonged scan time with multiple high SAR-sequences [37]. It is unclear if similar heating effects would occur in humans. However, we believe that - with an average scanning time of 33 minutes for whole body staging from which half of the scan time is spaced by low SAR sequences (e.g.: DWI and gradient T1 lung sequence) - the WB-DWI/MRI protocol lies within the proposed scan limitations. No adverse fetal effects could be directly linked to imaging in our patient group.

Contrary to using MRI itself, the American College of Radiology (ACR) paper on safe MR practices advises for extreme caution to use gadolinium [38]. Previous studies in non-pregnant cancer patients have shown that DWI reaches at least similar accuracy for detecting

primary tumors, nodal and distant metastases as would be achieved by gadolinium-enhanced MRI [10-12,30]. Taking into account prior studies and our data, we believe that the use of DWI can reliably obviate the need for gadolinium contrast for staging during pregnancy.[39] The certainty to cover the entire body in a single examination likely contributed to the higher accuracy of WB-DWI/MRI over conventional staging. However, the improved detection rate of metastases may come at the cost of decreased specificity [7]. We could largely overcome this problem by correlating DWI to the co-registered anatomical T2- and T1-weighted sequences, seen the similar specificity found between WB-DWI/MRI and conventional staging. Moreover, only one additional CT of the ribcage was requested by 1 reader for a false positive WB-DWI/MRI reading of a skeletal hemangioma with T2 shine-through [7].

We acknowledge three limitations of this study. First, we could only include a low number of patients, which impacted most on the low number of patients with distant metastases reflected by the large ranges of confidence intervals. This directly results from the single center study setting in a patient population with low cancer incidence. However, to the best of our knowledge, current literature only consists of two case reports. Vermoolen et al reported the case of a woman with Hodgkin lymphoma at 31w of gestation [40]. WB-MRI, performed with coronal T1 and STIR T2-weighted acquisitions, found cervical and mediastinal lymph node involvement. Montagna et al reported the case of a pregnant woman with breast cancer; WB-DWI/MRI showed the breast nodule, axillary involvement, and bone metastases [41]. Second, WB-DWI/MRI was performed irrespective of clinical risk of distant metastatic spread. One could argue that WB-DWI/MRI is not indicated to assess Tis-T1 breast cancer, as was done in this pilot study. However, the purpose of this study was primarily to assess sensitivity and specificity of WB-DWI/MRI, justifying the inclusion of these patients. We acknowledge that further validation of WB-DWI/MRI in a larger patient population and in

multicenter study setting is preferable. Third, even though the negative DWI/MRI findings in the lungs in this study were corroborated by the absence of lung metastases during the entire follow-up period, it is still possible that due to the resolution limitations of DWI/MRI millimetric deposits could have been missed. In case of doubt, a non-contrast chest CT examination could be considered.

In conclusion, WB-DWI/MRI is feasible for single-step non-invasive staging of cancer during pregnancy with good to excellent reader reproducibility and shows additional value to conventional imaging procedures for detecting distant and nodal metastases. If established for staging during pregnancy, WB-DWI/MRI could obviate the need of radiation, contrast-injection or multiple diagnostic tests. This is better in terms of oncologic staging, time management, financial costs, prevention of fetal radiation exposure, and emotional burden for the patient.

Acknowledgments: FA is senior researcher for the Research Fund Flanders (F.W.O.). Supported by grants from the Belgian Cancer Plan (Ministry of Health), Stichting tegen Kanker, and the CRADLE project supported by the European Research Council.

Reference List

1.Pavlidis NA (2002) Coexistence of pregnancy and malignancy. Oncologist 7(4):279-287.

2.Berkowitz GS, Skovron ML, Lapinski RH, Berkowitz RL (1990) Delayed childbearing and the outcome of pregnancy. N Engl J Med 322(10):659-664.

3.Stensheim H, Moller B, van Dijk T, Fossa SD (2009) Cause-specific survival for women diagnosed with cancer during pregnancy or lactation: a registry-based cohort study. J Clin Oncol 27(1):45-51.

4.Kanal E, Barkovich AJ, Bell C, et al (2013) ACR guidance document on MR safe practices: 2013. J Magn Reson Imaging 37(3):501-530.

5. Woussen S, Lopez-Rendon X, Vanbeckevoort D, Bosmans H, Oyen R, Zanca F (2016) Clinical indications and radiation doses to the conceptus associated with CT imaging in pregnancy: a retrospective study. Eur Radiol 26(4):979-85.

6.Michielsen K, Vergote I, Op de Beeck K, et al (2014) Whole-body MRI with diffusion-weighted sequence for staging of patients with suspected ovarian cancer: a clinical feasibility study in comparison to CT and FDG-PET/CT. Eur Radiol 24(4):889-901.

7.Koh DM, Collins DJ (2007) Diffusion-weighted MRI in the body: applications and challenges in oncology. AJR Am J Roentgenol 188(6):1622-1635.

8.Petralia G, Padhani A, Summers P, et al (2013) Whole-body diffusion-weighted imaging: is it all we need for detecting metastases in melanoma patients? Eur Radiol 23(12):3466-3476.

9.Mayerhoefer ME, Karanikas G, Kletter K, et al (2015) Evaluation of Diffusion-Weighted Magnetic Resonance Imaging for Follow-up and Treatment Response Assessment of Lymphoma: Results of an 18F-FDG-PET/CT-Controlled Prospective Study in 64 Patients. Clin Cancer Res 21(11):2506-2513.

10. de Bondt RB, Nelemans PJ, Hofman PA, et al (2007) Detection of lymph node metastases in head and neck cancer: a meta-analysis comparing US, USgFNAC, CT and MR imaging. Eur J Radiol 64(2):266-272.
11. Wu LM, Hu J, Gu HY, Hua J, Xu JR (2013) Can diffusion-weighted magnetic resonance imaging (DW-MRI) alone be used as a reliable sequence for the preoperative detection and characterisation of hepatic metastases? A meta-analysis. Eur J Cancer 49(2):572-584.
12. Li B, Li Q, Nie W, Liu S (2014) Diagnostic value of whole-body diffusion-weighted magnetic resonance imaging for detection of primary and metastatic malignancies: a meta-analysis. Eur J Radiol 83(2):338-344.
13. Sobin LH, Gospodarowicz MK, Wittekind C (2009) TNM Classification of Malignant Tumors, 7th Edition. Hoboken, NJ: Wiley-Blackwell
14. Klar N, Lipsitz SR, Leong T (2002) An exact bootstrap confidence interval for K in small studies. The Statistician 51(4):467-478.
15. Rao JN, Scott AJ (1992) A simple method for the analysis of clustered binary data. Biometrics 48(2):577-585.
16. Zou G, Donner A (2004) Confidence interval estimation of the intraclass correlation coefficient for binary outcome data. Biometrics 60:807-811.
17. Crump M, Goss PE, Prince M, Girouard C (1996) Outcome of extensive evaluation before adjuvant therapy in women with breast cancer and 10 or more positive axillary lymph nodes. J Clin Oncol 14(1):66-69.
18. Hilsenbeck SG, Ravdin PM, de Moor CA, Chamness GC, Osborne CK, Clark GM (1998) Time-dependence of hazard ratios for prognostic factors in primary breast cancer. Breast Cancer Res Treat 52(1-3):227-237.

19. Chung J, Youk JH, Kim JA, et al (2014) Role of diffusion-weighted MRI: predicting axillary lymph node metastases in breast cancer. Acta Radiol 55(8):909-916.
20. Luo N, Su D, Jin G, et al (2013) Apparent diffusion coefficient ratio between axillary lymph node with primary tumor to detect nodal metastasis in breast cancer patients. J Magn Reson Imaging 38(4):824-828.
21. Fornasa F, Nesoti MV, Bovo C, Bonavina MG (2012) Diffusion-weighted magnetic resonance imaging in the characterization of axillary lymph nodes in patients with breast cancer. J Magn Reson Imaging 36(4):858-864.
22. Scaranelo AM, Eiada R, Jacks LM, Kulkarni SR, Crystal P (2012) Accuracy of unenhanced MR imaging in the detection of axillary lymph node metastasis: study of reproducibility and reliability. Radiology 262(2):425-434.
23. Rautiainen S, Kononen M, Sironen R, et al (2015) Preoperative axillary staging with 3.0-T breast MRI: clinical value of diffusion imaging and apparent diffusion coefficient. PLoS One 10(3):e0122516.
24. Alvarez S, Anorbe E, Alcorta P, Lopez F, Alonso I, Cortes J (2006) Role of sonography in the diagnosis of axillary lymph node metastases in breast cancer: a systematic review. AJR Am J Roentgenol 186(5):1342-1348.
25. Ohno Y, Koyama H, Yoshikawa T, et al (2011) N stage disease in patients with non-small cell lung cancer: efficacy of quantitative and qualitative assessment with STIR turbo spin-echo imaging, diffusion-weighted MR imaging, and fluorodeoxyglucose PET/CT. Radiology 261(2):605-615.
26. Lavi N, Horowitz NA, Brenner B (2015) Author response: Precise staging of lymphoma duringpregnancy using MRI is not always crucial. Womens Health (Lond Engl) 11(2):103-104.

27. van Dam L, Han SN, Dierickx D, Amant F (2015) Optimal staging of lymphoma during pregnancy is crucial. Womens Health (Lond Engl) 11(2):101-102.
28. Clouse ME, Harrison DA, Grassi CJ, Costello P, Edwards SA, Wheeler HG (1985) Lymphangiography, ultrasonography, and computed tomography in Hodgkin's disease and non-Hodgkin's lymphoma. J Comput Tomogr 9:1-8.
29. Espada M, Garcia-Flores JR, Jimenez M, et al (2013) Diffusion-weighted magnetic resonance imaging evaluation of intra-abdominal sites of implants to predict likelihood of suboptimal cytoreductive surgery in patients with ovarian carcinoma. Eur Radiol 23(9):2636-2642.
30. Low RN, Sebrechts CP, Barone RM, Muller W (2009) Diffusion-weighted MRI of peritoneal tumors: comparison with conventional MRI and surgical and histopathologic findings--a feasibility study. AJR Am J Roentgenol 193(2):461-470.
31. Lecouvet FE, El Mouedden J, Collette L, et al (2012) Can whole-body magnetic resonance imaging with diffusion-weighted imaging replace Tc 99m bone scanning and computed tomography for single-step detection of metastases in patients with high-risk prostate cancer? Eur Urol 62(1):68-75.
32. Strizek B, Jani JC, Mucyo E, et al (2015) Safety of MR Imaging at 1.5 T in Fetuses: A Retrospective Case-Control Study of Birth Weights and the Effects of Acoustic Noise. Radiology 275(2):530-537.
33. Clements H, Duncan KR, Fielding K, Gowland PA, Johnson IR, Baker PN (2000) Infants exposed to MRI in utero have a normal paediatric assessment at 9 months of age. Br J Radiol 73(866):190-194.
34. Kok RD, de Vries MM, Heerschap A, van den Berg PP (2004) Absence of harmful effects of magnetic resonance exposure at 1.5 T in utero during the third trimester of pregnancy: a follow-up study. Magn Reson Imaging 22(6):851-854.

35. Reeves MJ, Brandreth M, Whitby EH, et al (2010) Neonatal cochlear function: measurement after exposure to acoustic noise during in utero MR imaging. Radiology 257(3):802-809.
36. Victoria T, Jaramillo D, Roberts TP, et al (2014) Fetal magnetic resonance imaging: jumping from 1.5 to 3 tesla (preliminary experience). Pediatr Radiol 44(4):376-386.
37. Cannie MM, De Keyzer F, Van Laere S et al (2015) Potential Heating Effect in the Gravid Uterus by Using 3-T MR Imaging Protocols: Experimental Study in Miniature Pigs. Radiology 151258.
38. The American College of Radiology (2010) Manual on Contrast Media, version 7.0: 81.
39. de Haan J, Vandecaveye V, Han SN, Van de Vijver KK, Amant F (2016) Difficulties with diagnosis of malignancies in pregnancy. Best Pract Res Clin Obstet Gynaecol 33:19-32
40. Vermoolen MA, Kwee TC, Nievelstein RA (2010) Whole-body MRI for staging Hodgkin lymphoma in a pregnant patient. Am J Hematol 85(6):443.
41. Montagna E, Peccatori F, Petralia G, Tomasi CN, Iorfida M, Colleoni M (2014) Whole-body magnetic resonance imaging, metastatic breast cancer and pregnancy: a case report. Breast 23(3):295-29

Tables and Figures

Table 1. Applied modalities for conventional staging versus WB-DWI/MRI

Patient ID	Conventional staging	WB-DWI/MRI
Patient 1	Breast ultrasound Mammography Chest X-ray Liver ultrasound MRI spine	Single step WB-DWI/MRI
Patient 2	Chest X-ray Liver ultrasound Pelvic MRI	Single step WB-DWI/MRI + dedicated pelvic sequences
Patient 3	MRI Liver Colonoscopy	Single step WB-DWI/MRI
Patient 4	Breast ultrasound Mammography MRI breasts Chest X-ray Liver ultrasound Bone scan Chest CT (low dose)	Single step WB-DWI/MRI
Patient 5	Breast ultrasound Mammography Chest X-ray Liver ultrasound MRI spine	Single step WB-DWI/MRI - Reader 2 Reader 1 additional CT scan of rib cage
Patient 6	Gynecological ultrasound	Single step WB-DWI/MRI
Patient 7	Pelvic MRI Staging lymphadenectomy	Single step WB-DWI/MRI + dedicated pelvic sequences
Patient 8	chest X-ray Ultrasound PET-CT	Single step WB-DWI/MRI
Patient 9	Breast ultrasound	Single step WB-DWI/MRI

	Mammography Chest X-ray Liver ultrasound	
Patient 10	Breast ultrasound Mammography Chest X-ray Liver ultrasound MRI breasts	Single step WB-DWI/MRI
Patient 11	Breast ultrasound Mammography	Single step WB-DWI/MRI
Patient 12	Breast ultrasound Mammography MRI breasts MRI spine	Single step WB-DWI/MRI
Patient 13	Breast ultrasound Mammography MRI breasts PET-CT (ultra-low dose)	Single step WB-DWI/MRI
Patient 14	Breast ultrasound Mammography MRI breasts MRI chest CT guided biopsy of mediastinal mass	Single step WB-DWI/MRI
Patient 15	MRI orbita	Single step WB-DWI/MRI
Patient 16	CT chest and abdomen Bone scan MR breast	Single step WB-DWI/MRI
Patient 17	Chest X-ray abdominal ultrasound	Single-step WB-DWI/MRI
Patient 18	Chest X-ray Chest CT liver ultrasound	Single-step WB-DWI/MRI
Patient 19	Breast ultrasound Mammography Chest X-ray	Single-step WB-DWI/MRI

	Liver ultrasound	
Patient 20	Chest X-ray Abdominal MRI (no DWI)	Single-step WB-DWI/MRI

Table 2. Overview of sequence parameters

DWI, diffusion weighted imaging; mDIXON, multi-echo 2-point Dixon; eTHRIVE, T1-weighted high-resolution isotropic volume excitation; TSE, turbo spin-echo imaging; STIR, short T1 inversion recovery; SPAIR, spectrally adiabatic inversion recovery.

	DWI **Transverse**	**T2-TSE** **Single-shot** **Coronal**	**T1-TSE** **Sagittal spine**	**T1-TSE** **Coronal pelvis**	**3D T1 gradient-echo** **Transverse lungs**
Image stations	4	3	2	1	1
Respiration	Free breathing	Free breathing	Free breathing	Free breathing	Breath-hold
Fat suppression	STIR (T1 = 250 ms)	None	None	None	SPAIR (eTHRIVE)
b-values (s/mm^2)	0-1000	None	None	None	None
Parallel imaging factor	2.5	4	2.5	2.5	2
Repetition time (ms)	8454	3000	400	500	3.2
Echo time (ms)	67	87	20	20	1.5
Slice thickness (mm)	5	6	4	4	1.5
Slice number	50/station	35/station	15	35	148
Intersection gap (mm)	0.1	0.6	0.4	0.4	0

Field of view (mm)	420 x 329	375 x 447	260 x 380	300 x 323	375 x 304
Acquired voxel size (mm)	4.57 x 4.71	1 x 1	1 x 1.3	0.74 x 0.81	1.49 x 1.5
Reconstructed voxel size (mm)	2.19 x 2.16	0.93 x 0.93	0.65 x 0.65	0.72 x 0.72	0.98 x 0.97
Signal averages	1	1	1	1	1
Imaging time (minutes)	17	2	6	3	0:15

Table 3. Disease extent and staging according to conventional staging, WB-DWI/MRI reader 1 and 2 and the reference standard.

Patient	Tumor type	Conventional staging	Staging WB-DWI/MRI		Reference standard staging
			Reader 1	Reader 2	
1	Breast cancer	T2N0M0	T2N1M0	T2N1M0	T2N1aM0
2	Cervical uterine cancer	FIGO Ib2 – T2aN1M0	FIGO Ib2 - T2aN1M0	FIGO IVb - T2aN1M1	FIGO IVb – T2aN0M1
3	Colon cancer	post-operative - T0N0M0	post-operative - T0N0M0	post-operative - T0N0M0	post-operative - T0N0M0
4	Breast cancer	T2N1M0	T2N3aM0	T2N3aM0	T2N3aM0
5	Breast cancer	T2N0M0	T2N1aM0	T2N1aM0	T2N1aM0
6	Borderline ovarian cyst	FIGO Ia	FIGO Ia	FIGO Ia	FIGO Ic
7	Cervical uterine cancer	post-conisation T0N0M0	post-conisation T0N0M0	post-conisation T0N0M0	post-conisation T0N0M0
8	Hodgkin's lymphoma	Ann-Arbor Stage II	Ann-Arbor stage II	Ann-Arbor stage II	Ann-Arbor stage II
9	Breast cancer	T3N0M0	T3N1aM0	T3N3aM0	T3aN1aM0
10	Paget breast	TisN0M0	T0N0M0	T0N0M0	TisN0M0
11	Breast cancer	T1N0M0	T1N0M0	T1N0M0	T1cN0M0
12	Breast cancer	T4N1M1	T4N1M1	T4N1M1	T4N1M1
13	Breast cancer	TxN1M0	T1N3bM0	T1N3cM0	T1N3cM0
14	Hodgkin's lymphoma	Ann Arbor Stage I	Ann Arbor Stage II	Ann Arbor Stage II	Ann Arbor Stage II
15	Conjunctival carcinoma	post-operative - T0N0M0	post-operative - T0N0M0	post-operative - T0N0M0	post-operative - T0N0M0
16	Breast cancer	[L] T3N1 - [R] T3N0 M0	[L] T3N1 - [R] T3N0 M0	[L] T3N1 - [R] T3N0 M0	[L] T3N1 - [R] T3N0 M0
17	Hodgkin's lymphoma	Ann-Arbor Stage III	Ann-Arbor Stage III	Ann-Arbor Stage III	Ann-Arbor Stage III
18	Lung cancer	T2aN0M0	T2aN1M0	T2aN0M0	T2aN0M0
19	Breast cancer	T2N0M0	T2N0M0	T2N0M0	T2N0M0
20	Colon cancer	T4aN0M0	T4aN0M1a	T4aN0M1a	T4aN0M1a

Table 4. Comparative sensitivities, specificities, accuracies, PPVs and NPVs of conventional staging and WB-DWI/MRI.
CI, confidence interval; TP, true positive; FP, false positive; TN, true negative; FN, false negative; PPV, positive predictive value; NPV, negative predictive value.
Diagnostic accuracy. CI: 95% confidence interval, based on the binomial distribution, unless stated otherwise. (*) Upper limit of CI based on the ratio estimator for the variance of clustered binary data.

Method	Lesion	TP	FN	FP	TN	% Sensitivity (CI)	% Specificity (CI)	% PPV (CI)	% NPV (CI)	% Accuracy (CI)
Conventional staging	Primary lesion	16	1	1	2	94.1 (71.3-99.9)	66.7 (9.4-99.2)	94.1 (71.3-99.9)	66.7 (9.4-99.2)	90.0 (68.3-98.8)
	Nodal metastases	10	10	0	180	50.0 (27.2-72.8)	100.0 (98.0-100.0)	100.0 (69.2-100.0)	94.7 (90.5-98.4)*	95.0 (91.0-98.3)*
	Distant metastases	1	2	0	17	33.3 (0.8-90.6)	100.0 (80.5-100.0)	100.0 (2.5-100.0)	89.5 (66.9-98.7)	90.0 (68.3-98.8)
WB-DWI Reader 1	Primary lesion	16	1	1	2	94.1 (71.3-99.9)	66.7 (9.4-99.2)	94.1 (71.3-99.9)	66.7 (9.4-99.2)	90.0 (68.3-98.8)
	Nodal metastases	20	0	1	179	100.0 (83.2-100.0)	99.4 (96.9-100.0)	95.2 (76.2-99.9)	100.0 (98.0-100.0)	99.5 (97.2-100.0)
	Distant metastases	2	1	1	16	66.7 (9.4-99.2)	94.1 (71.3-99.9)	66.7 (9.4-99.2)	94.1 (71.3-99.9)	90.0 (68.3-98.8)
WB-DWI Reader 2	Primary lesion	16	1	1	2	94.1 (71.3-99.9)	66.7 (9.4-99.2)	94.1 (71.3-99.9)	66.7 (9.4-99.2)	90.0 (68.3-98.8)
	Nodal metastases	20	0	3	177	100.0 (83.2-100.0)	98.3 (95.2-99.7)	87.0 (66.4-97.2)	100.0 (97.9-100.0)	98.5 (95.7 -99.7)
	Distant metastases	3	0	0	17	100.0 (29.2-100.0)	100.0 (80.5-100.0)	100.0 (29.2-100.0)	100.0 (80.5-100.0)	100.0 (83.2-100.0)

Figure 1: Patient with breast cancer.

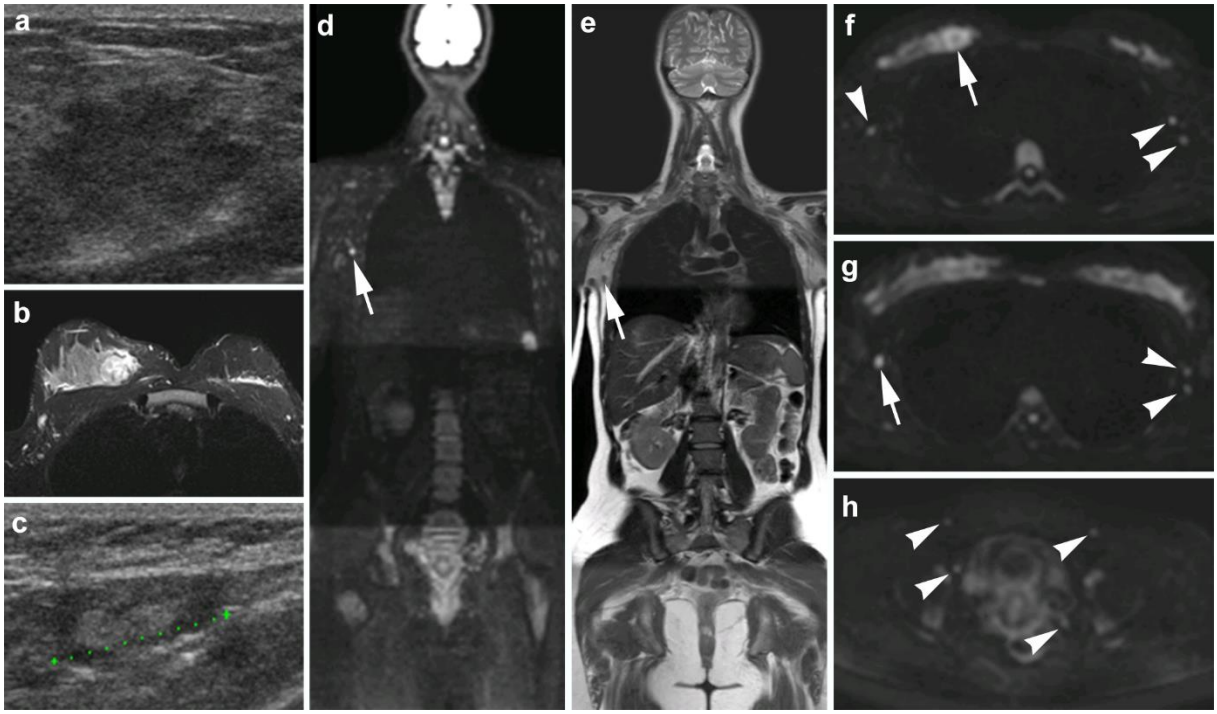

Caption: (A,B) Visualization of breast cancer by ultrasound and contrast-enhanced MRI. (C) Axillary ultrasound shows a lymph node with central hilum and regular cortex. Fine needle aspiration cytology did not show presence of malignant cells in the lymph node. Coronal WB-DWI/MRI consisting of a (D) b1000 WB-DWI sequence and (E) WB T2-weighted sequence shows a small axillary lymph node with b1000 increased signal (arrow). (F) Transverse b1000 DWI image shows (arrow) the right breast cancer characterized by increased signal intensity to the surrounding breast tissue. (G) As on the coronal image, the right axillar lymph node (arrow) shows increased signal intensity, similar to the breast cancer. (F,G,H) Arrowheads indicate axillar, inguinal and pelvic lymph nodes with lower signal intensity, considered as normal. Histopathology during a sentinel procedure confirmed the presence of a right axillar lymph node metastasis. The lymph nodes at other regions did not show any sign of progression during follow-up.

Figure 2: Patient with cancer of the transverse colon (A, B, C: asterisk).

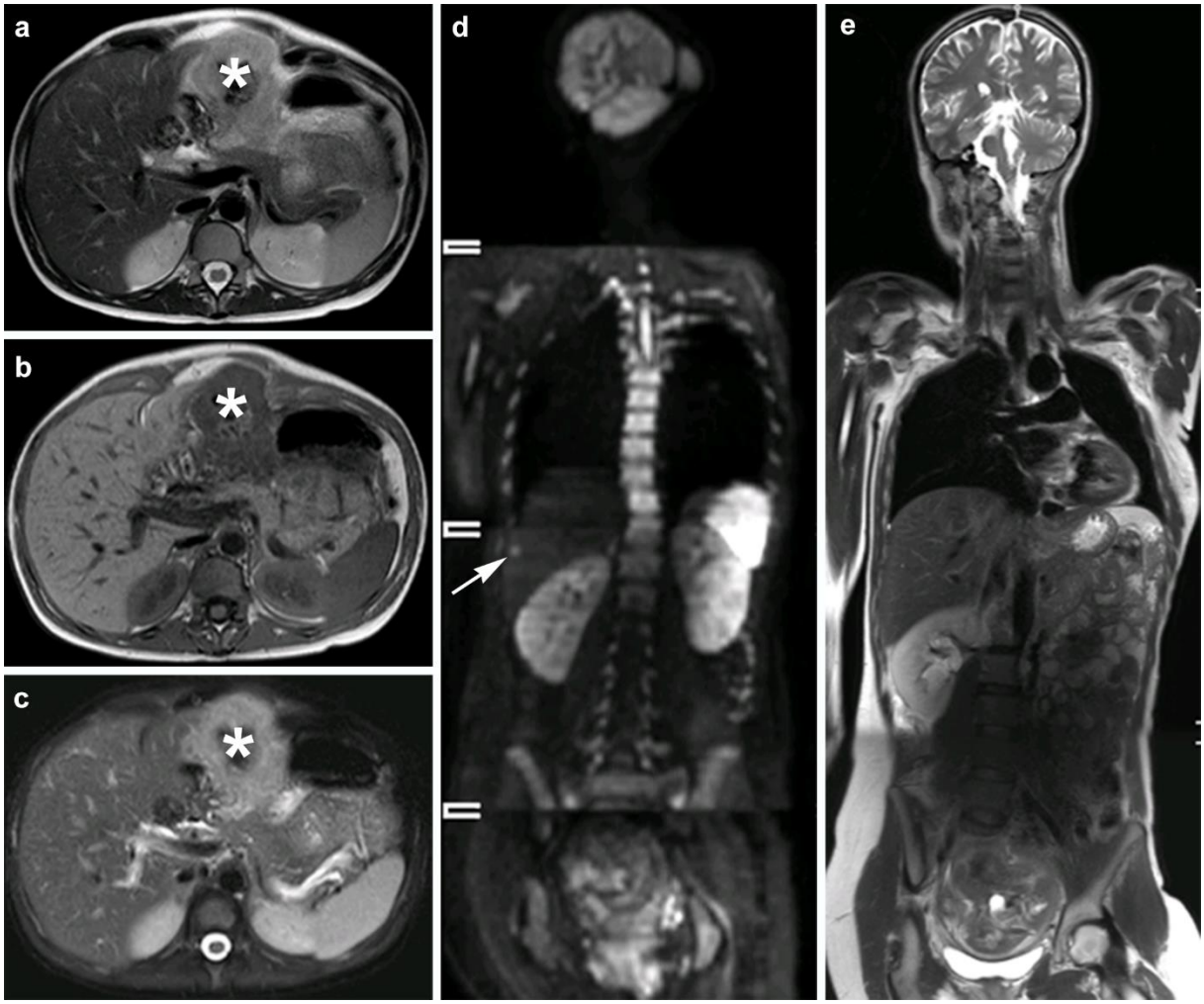

Conventional MRI of the abdomen performed at time of diagnosis for which a T2-weighted sequence without (A) and with (C) fat suppression and (B) T1-weighted sequence were performed reveals no liver lesions. (D) WB-WI shows a b1000 hyperintense lesion corresponding to the lateral subcapsular area of segment 6/7 of the liver on (E) the WB T2-weighted image compatible with a liver metastasis and was confirmed during surgery.

Figure 3: Patient with cervical uterine cancer.

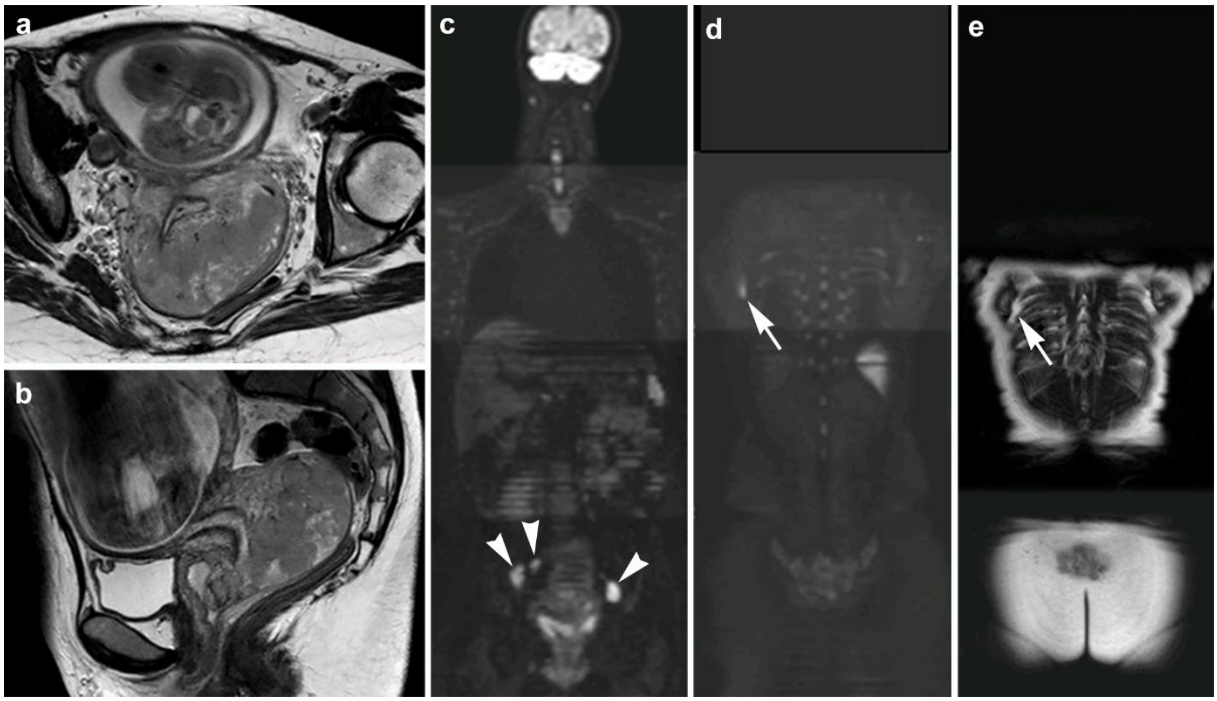

T2 weighted image in the (A) transverse and (B) sagittal plane shows an exophytic tumoral mass from the exocervix. (C) WB-DWI shows bilateral iliac lymphadenopathies (dashed arrows). (D) WB-DWI shows a hyperintense lesion corresponding to the inferior angle of the scapula at the corresponding (E) T2-weighted image compatible with a skeletal metastasis (arrows).